



Free
Magnet Offer



Copper Regulates the Canonical NLRP3 Inflammasome

Nikolaus Deigendesch, Arturo Zychlinsky and Felix Meissner

This information is current as of July 5, 2019.

J Immunol 2018; 200:1607-1617; Prepublished online 22 January 2018;

doi: 10.4049/jimmunol.1700712

<http://www.jimmunol.org/content/200/5/1607>

Supplementary Material <http://www.jimmunol.org/content/suppl/2018/01/22/jimmunol.1700712.DCSupplemental>

References This article **cites 70 articles**, 20 of which you can access for free at: <http://www.jimmunol.org/content/200/5/1607.full#ref-list-1>

Why *The JI*? Submit online.

- **Rapid Reviews! 30 days*** from submission to initial decision
- **No Triage!** Every submission reviewed by practicing scientists
- **Fast Publication!** 4 weeks from acceptance to publication

**average*

Subscription Information about subscribing to *The Journal of Immunology* is online at: <http://jimmunol.org/subscription>

Permissions Submit copyright permission requests at: <http://www.aai.org/About/Publications/JI/copyright.html>

Email Alerts Receive free email-alerts when new articles cite this article. Sign up at: <http://jimmunol.org/alerts>

The Journal of Immunology is published twice each month by The American Association of Immunologists, Inc., 1451 Rockville Pike, Suite 650, Rockville, MD 20852
Copyright © 2018 by The American Association of Immunologists, Inc. All rights reserved.
Print ISSN: 0022-1767 Online ISSN: 1550-6606.



Copper Regulates the Canonical NLRP3 Inflammasome

Nikolaus Deigendesch,* Arturo Zychlinsky,* and Felix Meissner†

Inflammasomes are multimeric protein complexes that are activated through a NOD-like receptor and regulate the proteolytic activation of caspase-1 and cytokines, like IL-1 β . The NLRP3 inflammasome is implicated in many human pathologies including infections, autoinflammatory syndromes, chronic inflammation, and metabolic diseases; however, the molecular mechanisms of activation are not fully understood. In this study we show that NLRP3 inflammasome activation requires intracellular copper. A clinically approved copper chelator, tetrathiomolybdate, inhibited the canonical NLRP3 but not the AIM2, NLRC4, and NLRP1 inflammasomes or NF- κ B-dependent priming. We demonstrate that NLRP3 inflammasome activation is blocked by removing copper from the active site of superoxide dismutase 1, recapitulating impaired inflammasome function in superoxide dismutase 1-deficient mice. This regulation is specific to macrophages, but not monocytes, both in mice and humans. In vivo, depletion of bioavailable copper resulted in attenuated caspase-1-dependent inflammation and reduced susceptibility to LPS-induced endotoxic shock. Our results indicate that targeting the intracellular copper homeostasis has potential for the treatment of NLRP3-dependent diseases. *The Journal of Immunology*, 2018, 200: 1607–1617.

Inflammation is a fundamental mechanism in maintaining homeostasis in response to tissue damage and invading pathogens. Innate immune sensors constantly survey organisms for signs of dyshomeostasis or the presence of foreign molecules to initiate adequate responses. Inflammasomes are intracellular multiprotein complexes consisting of a sensor protein of the AIM2-like or NOD-like receptor (NLR) families, the adaptor molecule apoptosis associated speck-like protein containing a CARD (ASC), and the IL-1 β processing cysteine protease caspase-1 (1–3). The assembly of inflammasomes is triggered by a wide range of molecules during infection, tissue damage, or alterations of cellular homeostasis (1, 4). Upon formation of inflammasomes, caspase-1 proteolytically cleaves different proteins, including the proforms of IL-1 β and IL-18, into active cytokines and facilitates their release by nonclassical secretion (5). IL-1 β is a master cytokine of local and systemic inflammation and plays a central role in a growing list of human diseases (6, 7). IL-1 β binds to the IL-1 receptor in target cells and induces more inflammatory mediators

(8). IL-1 β and IL-18 also promote the generation and maintenance of IFN- γ - and IL-17-producing T cells, which has implications for autoimmune disorders such as multiple sclerosis and type 1 diabetes (9). Independently from cytokine processing, caspase-1 also induces inflammatory cell death, named pyroptosis (10–12).

NLRP3 is an intracellular signaling molecule belonging to the NLR family, activated by a wide range of chemically diverse pathogen- and host-derived factors (4, 13). The exact mechanism of NLRP3 activation remains unclear despite extensive research. Published data suggest that the NLRP3 inflammasome is activated by potassium efflux, lysosomal destabilization or mitochondrial dysfunction (4). The regulation of the NLRP3 inflammasome by redox-related mechanisms, however, is controversial (2, 14–18).

Intriguingly, lowering bioavailable copper attenuates inflammation, and inhibits angiogenesis and tumor cell proliferation in various cancer models in vitro and in vivo; however, the underlying mechanisms are not well understood (19–21). We investigated the impact of copper-chelating drugs on inflammatory reactions and found that tetrathiomolybdate (TTM), which complexes copper by forming a tripartite bond with this cation and protein (22), specifically inhibits NLRP3 inflammasome activation. Copper depletion abrogates canonical NLRP3, but not other inflammasomes in macrophages by chelating this cation specifically from superoxide dismutase 1 (SOD1), which blocks its enzymatic activity and thereby alters the intracellular redox milieu (20). Importantly, copper is required for inflammasome activation in vivo because TTM treatment protects mice from LPS-induced endotoxic shock. Our data reveal a hitherto unknown copper-dependent regulatory mechanism for NLRP3 inflammasome activation in macrophages. Because treatment with TTM is approved for clinical use, for example for patients with Wilson's disease (23), our results open the door for novel anti-inflammatory treatment strategies for a wide range of NLRP3-mediated diseases.

*Department of Cellular Microbiology, Max Planck Institute for Infection Biology, D-10117 Berlin, Germany; and †Experimental Systems Immunology Laboratory, Max Planck Institute of Biochemistry, D-82152 Martinsried, Germany

ORCID: 0000-0003-1000-7989 (F.M.).

Received for publication May 22, 2017. Accepted for publication January 2, 2018.

N.D., A.Z., and F.M. designed experiments, analyzed data, and wrote the manuscript; F.M. conceived the study and supervised it together with A.Z.; N.D. performed experiments.

Address correspondence and reprint requests to Arturo Zychlinsky or Dr. Felix Meissner, Department of Cellular Microbiology, Max Planck Institute for Infection Biology, Charitéplatz 1, D-10117 Berlin, Germany (A.Z.) or Experimental Systems Immunology Laboratory, Max Planck Institute of Biochemistry, Am Klopferspitz 18, D-82152 Martinsried, Germany (F.M.). E-mail addresses: zychlinsky@mpiib-berlin.mpg.de (A.Z.) or meissner@biochem.mpg.de (F.M.).

The online version of this article contains supplemental material.

Abbreviations used in this article: ASC, apoptosis associated speck-like protein containing a CARD; BMDM, bone marrow-derived macrophage; CTxB, cholera toxin, subunit B; GSH, reduced glutathione; GSSG, glutathione disulfide (oxidized GSH); iNOS, inducible NO synthase; LDH, lactate dehydrogenase; LTx, lethal toxin from *Bacillus anthracis*; MOI, multiplicity of infection; NAC, *N*-acetyl-cysteine; NLR, NOD-like receptor; NOX2, NADPH-oxidase 2; PM, peritoneal macrophage; poly(dA:dT), poly(deoxyadenylic-desoxythymidyl); ROS, reactive oxygen species; SOD1, superoxide dismutase 1; TTM, tetrathiomolybdate.

Copyright © 2018 by The American Association of Immunologists, Inc. 0022-1767/18/\$35.00

Mice

SOD1- and NLRP3-deficient mice were purchased from the Jackson Laboratory on a C57BL/6 background or for more than 10 generations backcrossed on a C57BL/6 background. Caspase-1/11-deficient mice were obtained from BASF. All mice were housed under specific pathogen-free conditions in the animal facility of the Max Planck Institute for Infection Biology, Berlin. All mouse experiments were carried out in the S2 area of the Max Planck Institute for Infection Biology, Berlin, with sex- and age-matched 8–12 wk old mice. Experiments were done in accordance with the German Animal Protection Law and approved by the Landesamt für Gesundheit und Soziales, Berlin (G0064/12).

Isolation of human macrophages from ascites fluid

Ascites fluid from therapeutic paracentesis from patients with chronic ascites in the department of gastroenterology at the Charité, Berlin, was anonymously obtained in accordance with the Charité ethics committee. Ascites fluid was spun at 200 g for 15 min and the cellular pellet was resuspended in PBS containing 2 mM EDTA and 100 U/ml penicillin/streptomycin. The cell suspension was layered on Histopaque 1077 (Sigma-Aldrich) and centrifuged for 40 min at $400 \times g$. The mononuclear cell layer was aspirated, washed, and cultivated in DMEM supplemented with 2% (v/v) human serum, 2 mM L-glutamine, penicillin/streptomycin, and 10 mM HEPES on cell culture petri dishes for adherent cells. After 2 h, the nonadherent cells were washed off. The purity of cells was determined by FACS.

Isolation of human blood-derived monocytes

Blood from healthy volunteers was drawn in EDTA-coated vacutainers and diluted in PBS supplemented with 2 mM EDTA. Up to 30 ml of blood was layered on 15 ml of Histopaque 1077 and centrifuged at $400 \times g$ and 21°C for 30 min. The PBMCs were collected and washed with PBS/EDTA. Platelets were depleted by repeated centrifugation at $200 \times g$ for 15 min. Monocytes were isolated from PBMCs by negative selection using the Monocyte Isolation Kit II (Miltenyi Biotec) according to the manufacturer's instructions. Monocytes were cultivated in RPMI 1640 medium supplemented with 100 U/ml penicillin/streptomycin and 5% human serum (Sigma-Aldrich), and used for experiments the next day. For the experiments with monocyte-derived macrophages, monocytes were differentiated into macrophages in M1 or M2 differentiation medium (Promo Cell) for 6 d. Purity of monocytes and macrophages was more than 96% as determined by a fluorescent-activated cell sorter using anti-CD14 Ab (Miltenyi Biotec).

Isolation and generation of murine myeloid cells

For peritoneal macrophages, mice were injected with 1 ml of sterile 6% (w/v) thioglycolate solution and cells were harvested by peritoneal lavage with prewarmed sterile PBS 5 d later. Cells were washed and erythrocytes were isotonicly lysed at room temperature. Macrophages were cultured in DMEM supplemented with 10% (v/v) heat-inactivated FCS, 100 U/ml penicillin/streptomycin, and 2 mM L-glutamine under standard conditions at 37°C and 5% (v/v) CO₂, and adherent cells were used for experiments after overnight incubation. In vitro assays were performed in DMEM containing 2% FCS. Bone marrow-derived macrophages (BMDMs) were prepared from the femurs of mice and cultivated with DMEM containing 10% FCS, 10 mM HEPES, 1 mM pyruvate, 10 mM L-glutamine, and 20% M-CSF-conditioned medium derived from L929 fibroblast cultures. The cells were incubated at 37°C and 5% CO₂, and macrophages were harvested after 6 d in culture. Murine PBMCs were purified by drawing maximum 100 µl of blood per animal and layered onto Histopaque 1077, and centrifuged for 30 min at room temperature at $400 \times g$.

Inflammasome activation assays in vitro

Cells were seeded at 1×10^6 per ml in DMEM supplemented with 10% FCS, 2 mM L-glutamine, 100 U/ml penicillin/streptomycin, 10 mM HEPES, and incubated at 37°C with 5% CO₂. Cells were primed with 500 ng/ml ultra-pure LPS (*Salmonella typhimurium*, S-form LPS; Enzo Life Sciences) for 3 h and subsequently stimulated with ATP (5 mM) or nigericin (10 µM) for 1 h or the indicated period of time, silica (100 µg/ml) for 90 min or lethal toxin from *Bacillus anthracis* (LTx) at 1 µg/ml for each compound, lethal factor and protective Ag, recombinantly expressed in *Escherichia coli* BL21 (DE3), and affinity purified for 2 h. To study the AIM2 inflammasome, cells were transfected with poly(desoxyadenylic-desoxythymidylic) acid [poly(dA:dT)] using Lipofectamine 2000 (Life Technology) at a concentration of 1 µg DNA plus 3 µl Lipofectamine per milliliter. Supernatants were collected 3 h after transfection. As control,

independent wells were treated with transfection reagent in the same concentration without poly(dA:dT). To activate caspase-11 via the alternative pathway, cells were primed for 3 h with 500 ng/ml synthetic triacetylated lipoprotein (Pam3CSK4; Life Technology), a TLR1/2 ligand, prior to stimulation with 20 µg/ml cholera toxin, subunit B (CTxB), and 10 µg/ml LPS (*E. coli*, serotype O111:B4; Sigma-Aldrich). Supernatants were collected after 8 or 16 h. Supernatants were removed and analyzed using ELISA (DuoSet; R&D Systems). Lactate dehydrogenase (LDH) release was measured using the CytoTox96 nonradioactive cytotoxicity assay (Promega). Lysed cells in medium with 1% Triton X-100 served as a reference for maximal cell death. For bacterial infections with *E. coli* (at multiplicity of infection [MOI] 50), *Citrobacter rodentium* (at MOI 50) or *Shigella flexneri* (M90T; at MOI 25) cells were incubated for 90 min, before medium was supplemented with 100 µg/ml gentamicin (Life Technologies). For quantification of ASC specks, immortalized murine macrophages expressing transgenic ASC-mCherry fusion protein were primed with LPS and stimulated as indicated in albumin-precoated low bind tubes, and fixed with paraformaldehyde. The fixed cells were measured and quantified using an AMNIS imaging flow cytometer (Merck Millipore).

For coimmunoprecipitation experiments, cells were stimulated as indicated and lysed in cold NP-40 lysis buffer (1% Tx-100, 50 mM Tris-HCl at pH 7.4, 150 mM NaCl) supplemented with Roche Complete Protease Inhibitor. Flag-tagged proteins were immunoprecipitated with Anti-FLAG M2 Magnetic Beads (M8823; Sigma-Aldrich). The cell lysates were incubated with the magnetic beads for 3 h at 4°C before being washed in a magnetic separator.

Immunoblotting

For cell lysates, supernatant of adherent cells was removed and cells were lysed in 1% Triton X-100 in PBS supplemented with protease inhibitor for 10 min on ice. Lysate was centrifuged at $10,000 \times g$ for 5 min and supernatants were decanted for further analysis. Cell culture supernatants were precipitated by the addition of equal volumes of methanol and 0.25 vol of chloroform, vortexed, and centrifuged 15 min at $16,000 \times g$. The interphase was precipitated with methanol, again vortexed, and centrifuged for 15 min at $16,000 \times g$. The pellet was dried at 55°C and suspended in Laemmli loading buffer and further subjected to gel electrophoresis. After transfer using a semidry or wet blotting system polyvinylidene difluoride membranes were blocked with 1% (w/v) BSA in PBS with 0.1% (v/v) Tween-20 for 1 h at room temperature. Membranes were incubated with primary Abs in PBS with 0.1% (v/v) Tween-20 with 0.1% (w/v) BSA and secondary Abs conjugated to HRP. For visualization membranes were incubated with ECL substrate (ECL Western Blot Substrate; Pierce) and the signal was detected with photographic films (Hyperfilm ECL; GE Healthcare). For reprobing, polyvinylidene difluoride membranes were incubated with stripping buffer (Restore Stripping Buffer; Pierce) for 30 min at room temperature and washed extensively before blocking and reprobing.

Reagents and Abs

Ultra-pure LPS from *S. typhimurium* (S-type) was from Enzo Life Sciences, LPS derived from *E. coli* (serotype O111:B4), and ATP was from Sigma-Aldrich. Nigericin and poly(dA:dT) was from InvivoGen; Lipofectamine 2000 and all cell culture reagents were purchased from Life Technology. Recombinant IFN-γ was from Miltenyi Biotec. The following Abs were used: mouse caspase-1 (kindly provided by P. Vandennebeele, Ghent), mouse IL-1β (ab9722; Abcam), mouse SOD1 (FI-154; Santa Cruz), mouse ASC (sc-22514-R; Santa Cruz), mouse phospho-p38 (9216; Cell Signaling), mouse p38 (9212; Cell Signaling), mouse IkBa (400 001; Calbiochem), mouse phospho-Erk (9101; Cell Signaling), mouse Erk (9102; Cell Signaling), mouse caspase-11 (clone 17D9; Novus Biologicals), and mouse NLRP3 (ab4207; Abcam). For immunoprecipitation experiments immunoblots were probed with Abs against NEK7 (ab133514 by Abcam) and NLRP3 (cryo2; AG-20B-0014, C100 by Adipogen).

Measurement of reactive oxygen species and glutathione

For detection of intracellular reactive oxygen species (ROS), cells were incubated for 20 min at 37°C with 10 µM CM-H2DCFDA (Molecular Probes), then washed with PBS and resuspended in RPMI 1640 with 0.5% (v/v) FCS without phenol red. Intracellular ROS was quantified by flow cytometry using a MACSQuant flow cytometer (Miltenyi Biotec) and data were analyzed with FlowJo Version 10. The concentration of reduced glutathione (GSH) was measured colorimetrically using the glutathione [glutathione disulfide (oxidized GSH)(GSSG)/GSH] detection kit (Enzo Life Sciences).

Immunofluorescence

Peritoneal macrophages were seeded on uncoated glass coverslips and cultivated overnight in DMEM supplemented with 10% (v/v) FCS, 100 U/ml penicillin/streptomycin, and 2 mM L-glutamine under standard conditions at 37°C and 5% (v/v) CO₂. Attached cells were primed and stimulated before fixation in 2% paraformaldehyde for 15 min at room temperature, then permeabilized with 0.1% Triton X-100 in PBS for 15 min at room temperature, and blocked in PBS with 2% BSA and 5% rat serum for 30 min. Cells were stained with monoclonal anti-ASC Ab from rat (clone 8E4.1) followed by Cy3-labeled secondary Abs (Jackson Laboratory). Finally, cells were counterstained with anti-CD11b-FITC-conjugated Abs (Miltenyi Biotec) and Hoechst 33258. Coverslips were mounted using ProLong Gold anti-fade mountant (Molecular Probes). Imaging was performed using a Leica TCS SP8 confocal microscope.

Histology

Murine spleens were fixed in 4% (w/v) paraformaldehyde in PBS and paraffin embedded. Paraffin sections 4 μm thick were stained using routine H&E staining or with Abs against cleaved caspase-3 (clone 5A1E; Cell Signaling) by using the iVIEW DAB Detection Kit (Ventana, Tucson, AZ) with biotinylated secondary Abs and diaminobenzidine visualization of the peroxidase reaction product with a Benchmark XT immunostainer (Ventana). For the TUNEL staining, spleens from treated mice were fixed at 4°C for 24 h in 4% (w/v) paraformaldehyde in PBS solution, washed with PBS, with a stepwise increased sucrose concentration from 10% per 24 h to 30% (w/v) sucrose in PBS. The sucrose-soaked spleens were embedded in Tissue-Tec OCT (Sakura) and cut in 7 μm slices using a cryomicrotome. The DeadEnd Fluorometric TUNEL System (Promega) was used according to the manufacturer's instructions to label fragmented DNA of apoptotic cells by catalytically incorporating fluorescein-12-dUTP at 3'-OH DNA ends using a terminal deoxynucleotidyl transferase. The fluorescein-12-dUTP-labeled DNA was visualized by fluorescence microscopy and quantified using Image J software.

LPS-induced endotoxic shock model

Age- and sex-matched mice were injected peritoneally with 15 mg/kg LPS derived from *E. coli* (serotype O111:B4; Sigma-Aldrich). The mice were monitored for signs of pain and severe suffering every 6 h. For cytokine measurements, an independent cohort of mice received 15 mg LPS per kilogram body weight and mice were anesthetized by inhalative isoflurane prior to blood draw from the retroorbital venous plexus into fast clotting serum tubes with separating gel (Becton Dickinson). Blood samples were incubated at room temperature for 10 min and centrifuged for 7 min at 10,000 × g and stored at -20°C. Cytokine concentrations were determined by ELISA or multiplex bead-based assays (Bio-Rad).

Statistical analysis

For technical replicates, data were plotted as mean plus SD. Biologically independent replicates were statistically analyzed by nonparametric (Mann-Whitney *U* test) or parametric tests (Student *t* test) as indicated and plotted as mean plus SEM. Paired datasets (e.g., time course of identical individuals) were analyzed by paired nonparametric tests. The survival of mice was analyzed by log-rank test. *p* < 0.05 was considered statistically significant.

Results

Depletion of bioavailable copper attenuates inflammasome activation in vivo

Because copper chelation was reported to attenuate LPS-induced responses (24), we tested the effect of TTM in a model of acute inflammation in vivo. We treated mice i.p. for 2 d with 20 mg/kg per day of this chelator before administering a lethal dose of 15 mg/kg LPS i.p. Caspase-1-dependent cytokines, such as IL-1β and the downstream inflammatory mediators IFN-γ and IL-17A, were significantly reduced in the serum of mice pretreated with copper chelator compared with untreated controls. In contrast, the caspase-1-independent cytokines RANTES, KC, and TNF were not affected by TTM pretreatment (Fig. 1A). Mice treated with this chelator were also significantly more resistant to endotoxic shock than untreated littermates. Notably, the survival rate of treated mice was comparable to mice deficient in caspase-1/11

(Fig. 1B). In addition, copper chelation significantly lowered free histone-DNA complexes and HMGB1 concentrations, which serve as sepsis markers (25, 26), in the serum 24 h after LPS injection (Fig. 1C). We also observed less lymphocyte apoptosis in the spleens of LPS-treated mice in combination with copper chelation (Fig. 1D) and confirmed the phenotype by staining the tissue sections for cleaved caspase-3, and visualized apoptotic cells using a TUNEL assay (Fig. 1D). Our data suggest that depletion of bioavailable copper specifically inhibits caspase-1 activation in vivo.

Copper is required for canonical NLRP3 inflammasome activation in vitro

We tested whether copper chelation downregulates caspase-1 activity in vitro. TTM strongly reduced IL-1β release from BMDMs in a dose-dependent manner after NLRP3 activation with ATP, nigericin, or silica (Fig. 1E). The calculated half-maximal inhibitory concentration was 4.07 μM for nigericin [IC₅₀ (95% confidence interval) 2.1–6.03], 5.18 μM for ATP (5.07–6.56), and 3.55 μM for silica (0.27–6.83) (Fig. 1E). Furthermore, copper chelation reduced the release of mature IL-18 and prevented pyroptosis in response to all three stimuli (Supplemental Fig. 1A–F). Caspase-1 activation was also sensitive to copper depletion as indicated by the absence of the autoproteolytic p20 fragment of caspase-1 in lysates of LPS-primed and NLRP3-activated BMDMs. However, priming was unaffected by copper depletion as indicated by comparable protein levels of pro-IL-1β and NLRP3 (Fig. 1F). Importantly, the inhibitory effect of TTM was completely reverted by adding divalent copper (Fig. 1G, Supplemental Fig. 1G), up to a TTM/metal ion molar ratio of 1:1. Other divalent metal ions did not show any effect on IL-1β secretion even at a 10 μM concentration (Supplemental Fig. 1G, 1H), demonstrating that TTM-mediated NLRP3 inhibition is copper specific.

Immunoblot analysis revealed that copper chelation did not affect phosphorylation of ERK and p38 MAPK, or degradation of IκB in BMDMs (Supplemental Fig. 2A). Importantly, caspase-1 activation was inhibited by copper chelation even in the absence of LPS priming in macrophages overexpressing NLRP3 (Supplemental Fig. 2B). Finally, secretion of KC, IL-6, and TNF was not copper sensitive in BMDMs activated with LPS and ligands to activate innate immune receptors, including the TLRs (Supplemental Fig. 2C). These data suggest that copper chelation specifically blocks caspase-1 activation without affecting NF-κB-dependent priming in BMDMs.

NLRP1, NLRC4, AIM2, and noncanonical inflammasomes do not require copper

We further evaluated whether copper is required for the activation of NLRP3-independent inflammasomes. Copper chelation did not affect IL-1β secretion or pyroptosis after activation of the AIM2 inflammasome by transfection of LPS-primed wild-type and NLRP3-deficient macrophages with the dsDNA analog poly(dA:dT) (Fig. 2A, 2B) (27–29). ATP and nigericin served as internal controls for NLRP3-dependent and copper-sensitive stimuli. We infected BMDM with virulent *S. flexneri* and observed that TTM did not block IL-1β or cell death, demonstrating that NLRC4 inflammasome activation does not require copper either (Fig. 2G) (30). Furthermore, LPS-primed wild-type BMDMs from mouse strains expressing functional NLRP1 alleles [such as BALB/c and 129-S2 (31)] released IL-1β and LDH in the presence of the copper chelator in response to recombinant LTx (Fig. 2H). Previous studies have shown that the TLR7 agonist imiquimod, a small molecule that blocks the quinone oxidoreductase NQO2, activates NLRP3 independent from K⁺ efflux (32, 33). Interestingly,

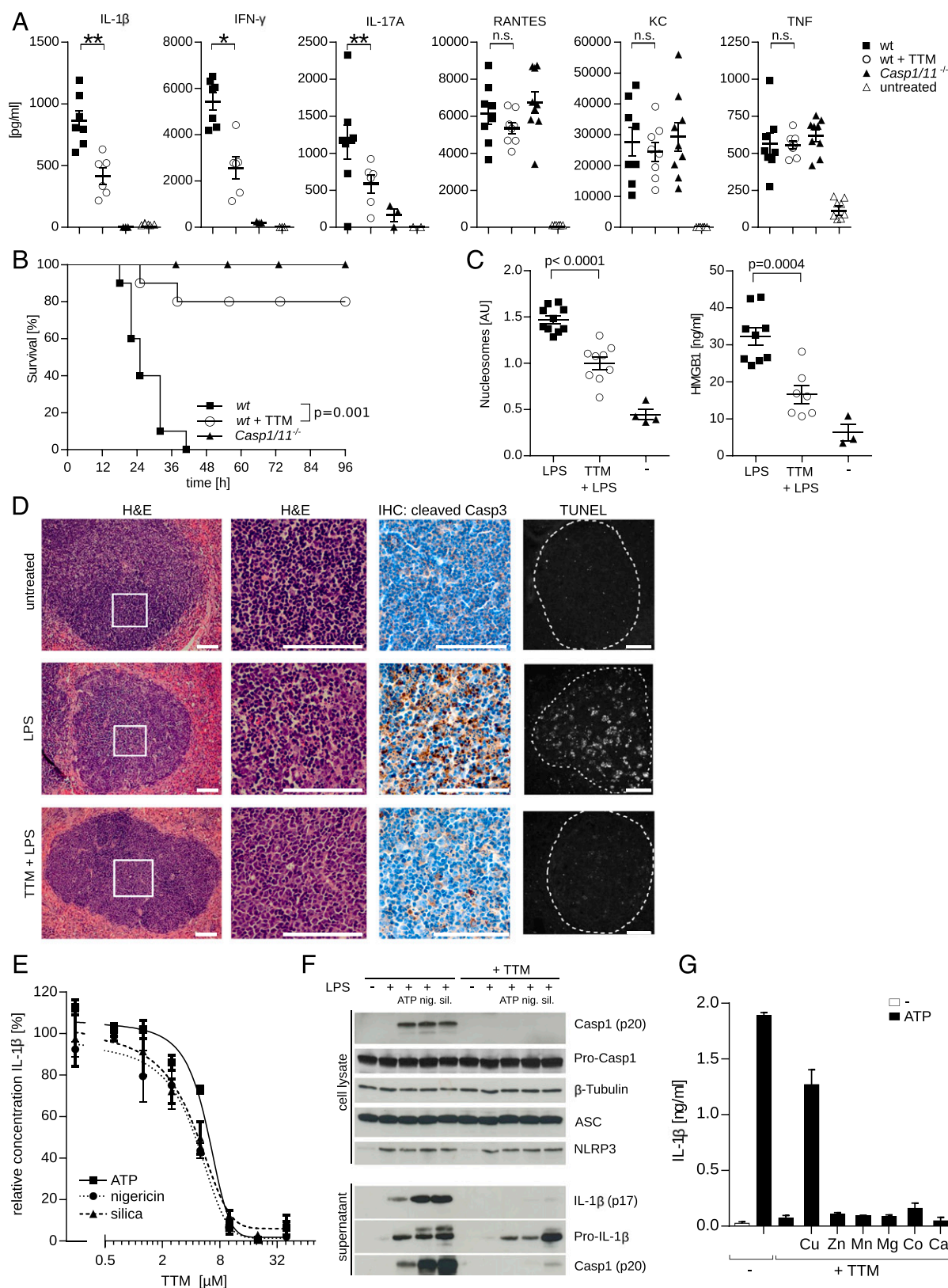


FIGURE 1. Depletion of bioavailable copper attenuates inflammasome activation in vivo and in vitro. **(A)** Serum concentrations of cytokines 8 h after i.p. LPS injection with and without pretreatment with TTM. Each symbol represents an individual animal. Statistics were calculated using Mann-Whitney *U* test, **p* < 0.05, ***p* < 0.01. **(B)** Survival of wild-type mice after treatment with TTM (*n* = 8) or vehicle control (*n* = 8) compared with caspase-1/11-deficient mice (*n* = 7) in LPS-induced shock (15 mg/kg per day i.p.). Statistics calculated using log-rank (Mantel-Cox) test. **(C)** Serum levels of nucleosomes and HMGB1 24 h after i.p. Each symbol represents an individual animal. **(D)** Representative histology from spleens of mice (*n* = 6 for each group) pretreated with TTM or vehicle control 24 h after i.p. LPS injection or left untreated. The paraformaldehyde-fixed and paraffin-embedded tissue was stained with H&E, or immunohistochemistry (IHC) was performed using Abs against cleaved caspase-3. TUNEL staining from cryo tissue sections shows apoptotic lymphocytes in the white pulp (dotted line). Scale bar, 100 μ m. **(E)** Secretion of IL-1 β from LPS-primed wild-type BMDMs pretreated with TTM (1–40 μ M) or left untreated and stimulated with ATP, nigericin, and silica. Data are calculated relative to levels without TTM (Figure legend continues)

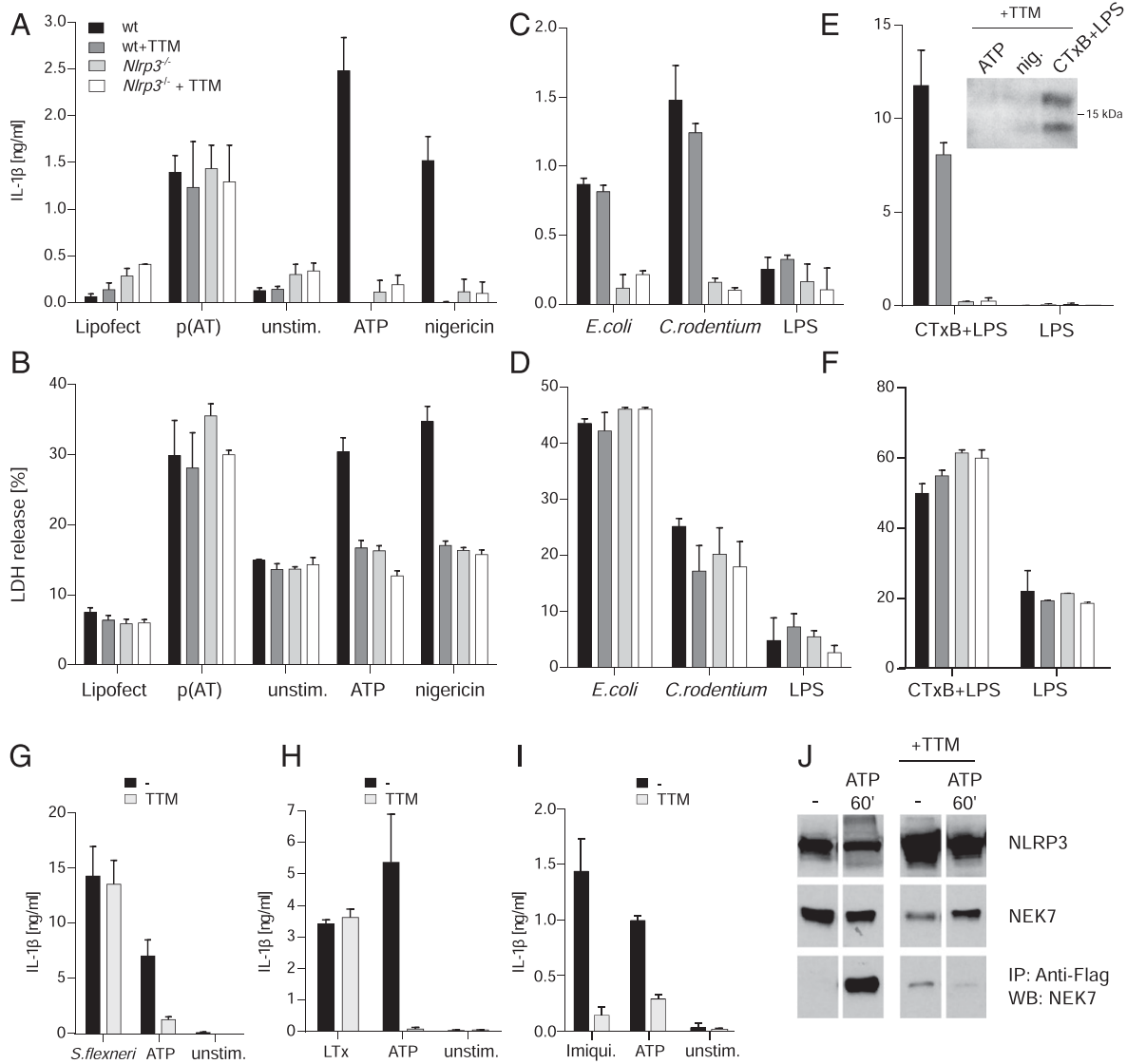


FIGURE 2. TTM specifically inhibits the canonical NLRP3 activation. Bar diagrams show means \pm SD of technical replicates, representative of at least three independently repeated experiments. (A and B) IL-1 β secretion and LDH release from LPS-primed wild-type and NLRP3-deficient BMDMs after incubation with or without TTM and stimulated with poly(dA:dT) [p(A:T)], ATP, or nigericin. Transfection reagent only (Lipofect) serves as control. (C and D) IL-1 β and LDH released from wild-type and NLRP3-deficient BMDMs pretreated with or without TTM and infected with *E. coli* or *C. rodentium* for 16 h (E and F) or treated with CTxB plus LPS or LPS only for 12 h. Western blot analysis of the supernatant of long-term incubation with CTxB confirms cleaved IL-1 β fragments. (G) IL-1 β released from BMDMs pretreated with or without TTM and infected with virulent *S. flexneri* at an MOI of 25 for 6 h. Stimulation with ATP was used as an internal control. (H) Supernatants from BMDMs treated with recombinant LTx for 6 h. (I) Supernatants of murine BMDMs stimulated with imiquimod for 2 h at 20 μ g/ml final concentration with and without TTM pretreatment. (D–I) Bars represent means \pm SD of technical replicates, representative of three independently repeated experiments. (J) Immortalized murine macrophages expressing transgenic Flag-tagged NLRP3 were treated as indicated and cell lysates were incubated with anti-Flag magnetic beads for immunoprecipitation. Supernatants and immunoprecipitation fractions were immunoblotted with Abs against NLRP3 and NEK7.

imiquimod-dependent NLRP3 inflammasome activation was also effectively blocked by TTM, suggesting that TTM acts upstream of NLRP3 activation on a target that is shared by different NLRP3 agonists (Fig. 2I). Therefore, we tested whether TTM blocks the association of NLRP3 and NEK7, a serine-threonine kinase recently identified upstream of NLRP3 inflammasome (34–36) activation. In

immunoprecipitation experiments with immortalized macrophages expressing transgenic NLRP3 (previously used, see Supplemental Fig. 2B), we accordingly observed a strongly reduced association of NLRP3 with NEK7 upon treatment with TTM (Fig. 2J).

Gram-negative bacteria, such as *E. coli* and *C. rodentium*, and intracellular LPS can be sensed by a noncanonical pathway, which

treatment (100%) and plotted as means \pm SD of technical triplicates; nonlinear regression analysis was performed. The data are representative of at least three independent experiments. (F) Immunoblots of cell lysates and supernatants from BMDMs primed and stimulated as indicated above, treated with or without 10 μ M TTM. (G) Secretion of IL-1 β from LPS-primed BMDMs pretreated with or without TTM in the presence of divalent cations at 10 μ M and stimulated with nigericin. Bars show means \pm SD of technical triplicates; the data are representative of three independent experiments.

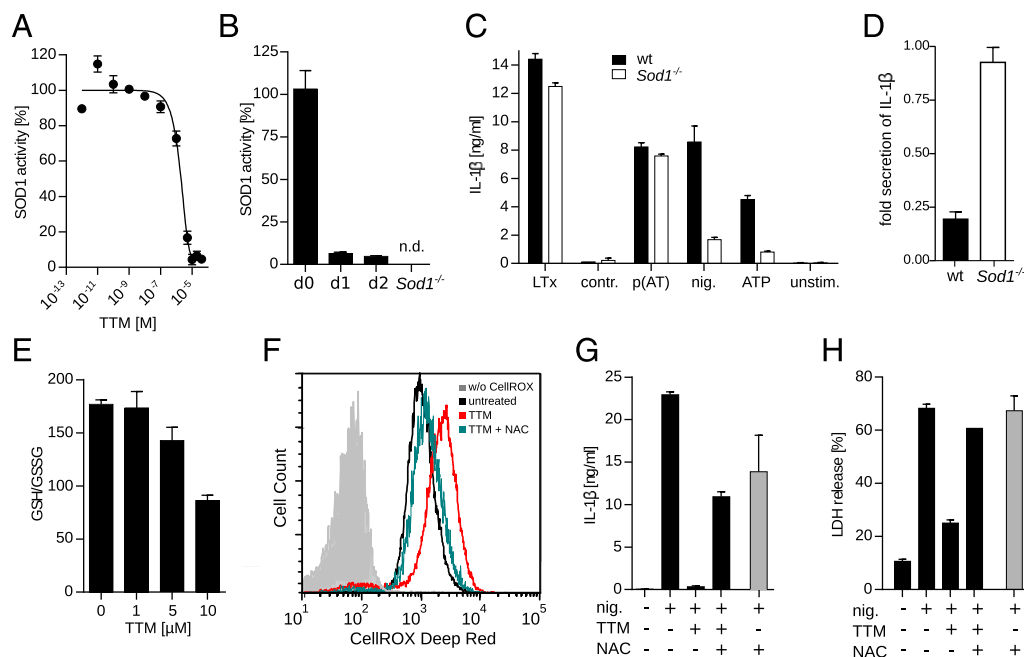


FIGURE 3. TTM acts through SOD1 inhibition. **(A)** SOD1 enzymatic activity measured in total cell lysates of wild-type BMDMs after pretreatment with 10 μ M TTM. Bars represent means \pm SD of technical triplicates, representative of three independently repeated experiments. **(B)** SOD1 enzymatic activity in erythrocyte lysates from wild-type mice before (day 0) and after one (day 1) or two (day 2) daily dosages of 20 mg/kg TTM i.p. ($n = 6$ animals per group). Erythrocyte lysates from SOD1-deficient mice served as controls. Bars are means \pm SEM relative to the enzymatic activity before TTM treatment (set to 100%). n.d., not detectable. **(C)** IL-1 β released from wild-type or SOD1-deficient PMs, LPS primed, and stimulated as indicated with LTx, poly(dA:dT) [p(A:T)], nigericin, or ATP or left stimulated. **(D)** IL-1 β released from wild-type or SOD1-deficient PMs incubated in the presence or absence of 10 μ M TTM, primed with LPS and stimulated with nigericin. The IL-1 β levels are plotted relative to IL-1 β secretion of PMs without TTM treatment. Bars represent means \pm SEM of PMs from individual animals ($n = 5$ each group). **(E)** Redox state of BMDMs incubated at increasing concentrations of TTM as indicated, plotted as the ratio of GSH to GSSG. Bars represent means \pm SD of three technical replicates. **(F)** Histogram of CellROX fluorescence intensity to determine intracellular reactive oxygen in BMDMs incubated with or without 10 μ M TTM and in the presence of NAC. Filled gray area, BMDMs without CellROX; untreated, BMDMs with CellROX, without TTM. **(G)** and **(H)** IL-1 β and LDH released from wild-type, LPS-primed BMDMs, treated as indicated with 10 μ M TTM and 20 mM NAC. Bars represent mean \pm SD of technical triplicates, representative of at least three independent experiments.

results in caspase-11-dependent cell death and NLRP3-dependent caspase-1 activation (37–40). We infected wild-type and NLRP3-deficient BMDMs with either *E. coli* or *C. rodentium* or treated cells with CTxB and LPS (*E. coli* serotype O111/B4) to test whether this noncanonical inflammasome activation is sensitive to copper depletion (Fig. 2C–F) (38–40). As previously reported (38), pyroptosis, but not IL-1 β maturation and release, was independent from NLRP3 in BMDMs (Fig. 2D, 2F). Notably, copper chelation did not inhibit the noncanonical activation of NLRP3 (Fig. 2C–F), indicating that distinct molecular mechanisms trigger canonical versus noncanonical NLRP3 activation. In accordance with previous reports (37, 41), procaspase-11 expression was induced by LPS priming; however, TTM did not affect the expression of this enzyme (Supplemental Fig. 2D). These data show that copper chelation blocks the canonical NLRP3 inflammasome specifically without affecting other tested inflammasomes.

Copper chelation inhibits SOD1 activity

TTM is a potent inhibitor of the copper-zinc-dependent SOD1 by removing the copper ion from the active site in cell-free conditions as well as in various nonmyeloid cells in vitro (20, 42, 43). Accordingly, the copper chelator inhibited the superoxide dismutase activity also in BMDMs in a dose-dependent manner (Fig. 3A). Aligning SOD1 activity and IL-1 β secretion (Fig. 1E) indicates that near-complete inhibition of SOD1 is required for the inhibition of NLRP3 activation. In vivo, a single i.p. dose of 20 mg/kg TTM in wild-type mice reduced SOD1 activity by \sim 95% in erythrocytes. The dismutase activity upon treatment with the copper chelator was almost as low as in erythrocyte lysates from SOD1-deficient mice (Fig. 3B).

We hypothesized that copper chelation abrogates inflammasome activation by inactivating SOD1. If this was true, deletion of SOD1 would inhibit the canonical NLRP3 inflammasome only. To test this, we elicited peritoneal macrophages (PMs) with thioglycolate because SOD1-deficient macrophages cannot be differentiated from BM precursor cells ex vivo. IL-1 β release (Fig. 3C) and pyroptosis (Supplemental Fig. 3A) were strongly reduced in SOD1-deficient PMs compared with wild-type macrophages treated with the canonical NLRP3 stimuli nigericin and ATP, as reported previously (44). In contrast, NLRP1 and AIM2 inflammasome activation were unaffected in SOD1-deficient cells (Fig. 3C, Supplemental Fig. 3A). Furthermore, IL-1 β secretion and cell death were similar in SOD1-deficient and wild-type PMs upon stimulation with CTxB, a noncanonical caspase-1/11 activator (Supplemental Fig. 3B) (38). Also, the activity of the NLRC4 inflammasome postinfection with virulent *S. flexneri* was comparable between wild-type and SOD1-deficient cells (Supplemental Fig. 3C).

SOD1 deficiency did not affect the expression of pro-IL-1 β (Supplemental Fig. 3D). Importantly, there was a strong reduction in the concentration of the active p20 fragment of caspase-1 in PMs stimulated with ATP and nigericin, but not upon stimulation with poly(dA:dT) or LTx (Supplemental Fig. 3D). Finally, the secretion of IL-6 and TNF after LPS stimulation was similar in SOD1-deficient and wild-type PMs (Supplemental Fig. 3E).

To rule out that the inhibitory effect of TTM was independent from superoxide dismutase activity, we treated SOD1-deficient PMs with this chelator. Copper depletion did not affect the residual activation of caspase-1 and IL-1 β cleavage in SOD1-deficient cells stimulated

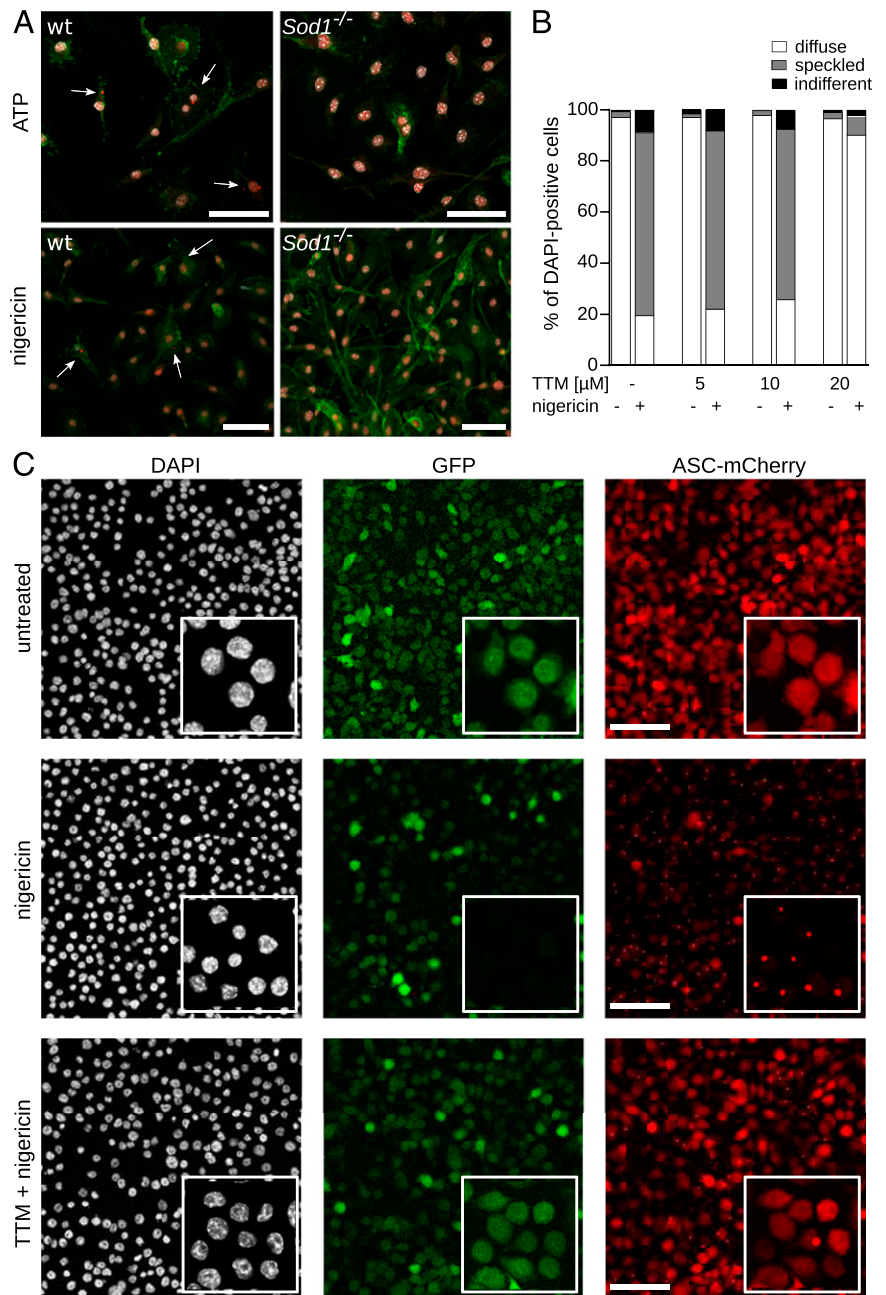


FIGURE 4. Superoxide blocks NLRP3-dependent ASC speck formation. **(A)** Representative fluorescent microscopy images of wild-type and SOD1-deficient PMs primed with LPS and stimulated with ATP and nigericin. Hoechst 33324 gray, Anti-CD11b green, and Anti-ASC red. Scale bar, 40 μ m. Arrows indicate intracellular ASC specks. **(B)** Quantification of intracellular ASC speck formation in DAPI-positive macrophages expressing transgenic ASC-mCherry with or without stimulation with nigericin at increasing TTM concentrations using imaging flow cytometry. **(C)** Confocal images of fixed and DAPI-stained macrophages expressing transgenic ASC-mCherry and enhanced GFP (eGFP) treated with 20 μ M TTM and nigericin as indicated. Scale bar, 50 μ m.

with nigericin or ATP (Fig. 3C), suggesting that TTM specifically attenuates caspase-1 activation by inhibiting SOD1 in macrophages (Fig. 3D). Our data collectively show that copper depletion specifically blocks canonical NLRP3 activation, phenocopying inflammasome downregulation in SOD1-deficient cells.

Copper depletion alters the intracellular redox state

SOD1 deficiency elevates the intracellular level of superoxide anions and alters the intracellular redox milieu (44, 45). To test whether redox alterations are mechanistically involved in the biological activity of copper chelation, we determined the ratio of GSH to GSSG as a proxy for the redox state in the cytoplasm (46, 47). Copper chelation shifted the intracellular GSH/GSSG ratio toward oxidation (Fig. 3E). To confirm this in a complementary approach we used CellROX, a fluorogenic probe that reports alterations of the intracellular redox milieu. Chelation of copper increased the fluorescent signal in BMDMs, and this was reversed by incubating cells with the cell-permeable ROS

scavenger *N*-acetyl-cysteine (NAC) (Fig. 3F). To link the altered redox state and the inhibition of IL-1 β secretion, we treated BMDMs with TTM and NAC before LPS priming and stimulating with nigericin. NAC antagonized the inhibitory effect of TTM on IL-1 β secretion and pyroptosis, indicating that copper chelation causes reversible redox alterations (Fig. 3G, 3H). Notably, in contrast to previously published data (48–50), high concentrations of NAC (up to 20 mM at pH-adjusted medium) had no effect on priming or inflammasome activation in our setting (Fig. 3G, 3H), and the cells were viable with an unaltered cytokine release upon LPS stimulation (Supplemental Fig. 4A, 4B).

As previously shown (14), treatment with diphenyliodonium, a commonly used inhibitor of NOX-dependent ROS production (51), blocked LPS priming efficiently; in contrast, diphenyliodonium treatment after LPS priming had no effect on inflammasome activation and did not affect TTM activity (Supplemental Fig. 4C). To obtain additional genetic evidence for the role of ROS generating and degrading enzymes in NLRP3 activation, we generated

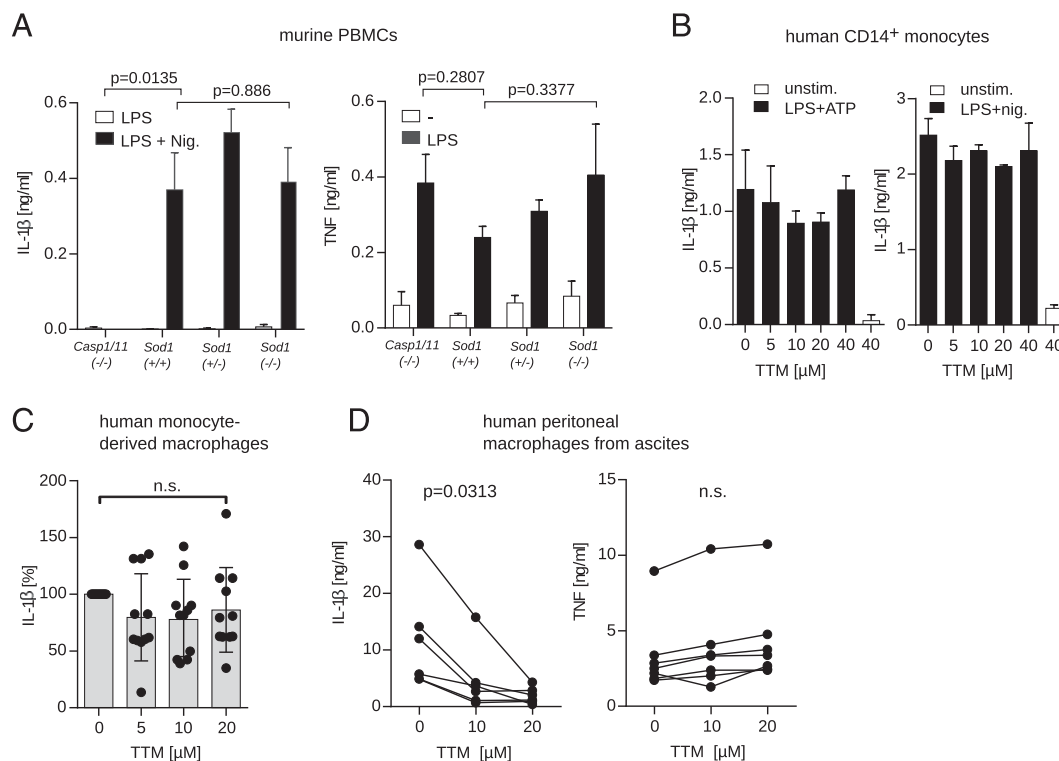


FIGURE 5. Redox sensitivity of NLRP3 activation is cell type dependent. **(A)** IL-1 β and TNF secretion of blood-derived PBMCs from wild-type, SOD1-deficient and caspase-1/11-deficient mice primed with LPS and stimulated with nigericin ex vivo. Data are plotted as means \pm SEM from at least four individual mice per genotype, p values calculated using Mann–Whitney U test. **(B)** IL-1 β secretion of human blood-derived CD14-positive monocytes, treated with increasing concentrations of TTM, primed with LPS, and stimulated with ATP or nigericin. Bars represent means \pm SD of technical triplicates, representative of at least three independent experiments with monocytes from different donors. **(C)** Relative IL-1 β secretion from human macrophage-like cells, in vitro differentiated from blood-derived monocytes, incubated with increasing concentrations of TTM, and LPS primed and stimulated with nigericin. **(D)** IL-1 β and TNF secretion from human peritoneal macrophages derived from ascites fluid, pretreated with TTM as indicated, LPS primed, and stimulated with nigericin. Statistics were calculated using a Mann–Whitney U test with pairwise comparison. (C and D) Each dot represents mean of one individual donor.

mice deficient for one or two alleles of both NADPH-oxidase 2 (NOX2) and SOD1. We activated BMDMs from these animals and show that the impaired release of mature IL-1 β from SOD1-deficient cells was not rescued by a deficiency in NOX2. Our genetic data thereby indicate that NOX2-derived ROS is dispensable for the redox-dependent abrogation of NLRP3 activation in our setting (Supplemental Fig. 4D).

We further investigated whether the SOD1-related phenotype was mechanistically linked to a recently proposed mechanism of NO-mediated suppression of the NLRP3 inflammasome via thiol nitrosylation (52, 53). Inducible NO synthase (iNOS, alternatively named NOS2) is the major source of NO in BMDMs after LPS and IFN- γ activation (Supplemental Fig. 4E). Copper chelation reduced the secretion of IL-1 β in iNOS-deficient BMDMs, pretreated with LPS and IFN- γ (Supplemental Fig. 4F), suggesting that TTM blocks the NLRP3 inflammasome through NO-independent mechanisms.

The cellular redox state regulates NLRP3-dependent ASC speck formation

Upon activation, the adapter protein ASC assembles into a large protein complex, termed speck, a key event in NLRP3 inflammasome activation (54, 55). We detected fewer cytoplasmic ASC-specks in SOD1-deficient macrophages after LPS priming and stimulation with ATP and nigericin compared with wild-type PMs (Fig. 4A). However, we did not observe differences in ASC speckling after transfection with poly(dA:dT). Because quantitative analyses were technically difficult in primary macrophages stained with Abs, we used an imaging flow cytometer to quantify

ASC specks in immortalized macrophages constitutively expressing ASC fused to the red fluorescent protein mCherry (56). These cells also express high levels of transgenic NLRP3 and therefore do not require priming. Copper chelation reduced ASC speck formation upon stimulation with nigericin (Fig. 4B, 4C). Inflammasome activation in response to transfection with poly(dA:dT) was insensitive to copper depletion. These data locate the requirement of copper for canonical NLRP3 activation upstream of ASC speckling.

Redox sensitivity of NLRP3 activation is cell type dependent

Distinct myeloid cells vary in redox regulation (57, 58). Hence, we compared the redox sensitivity of the NLRP3 inflammasome in macrophages and monocytes of both mice and humans. Interestingly, PBMCs from wild-type and SOD1-deficient mice, in contrast to caspase-1/11-deficient mice, released comparable amounts of IL-1 β upon LPS priming and stimulation with nigericin ex vivo (Fig. 5A). In PBMCs the greatest quantity of IL-1 β comes from monocytes. As expected, TNF secretion was comparable in SOD1-deficient, wild-type and caspase-1/11-deficient monocytes (Fig. 5A). Accordingly, copper chelation did not affect secretion of IL-1 β from human blood-derived CD14^{high}-monocytes stimulated with LPS only (data not shown) or primed with LPS and stimulated with ATP or nigericin (Fig. 5B). Furthermore, the IL-1 β secretion of human monocyte-derived macrophages was not sensitive to copper depletion (Fig. 5C). In addition, the IL-1 β secretion of the myeloid cell lines Mono Mac 6, THP-1, and U937 was also not reduced upon treatment with the copper chelator in vitro (data not shown). To test the effect of TTM in human

macrophages, we isolated PMs from patients suffering from a noninfectious accumulation of ascites fluid. The cells were isolated over a density gradient and plated overnight on cell culture dishes. Nonadherent cells were washed off. Cells from seven independent donors were incubated with or without TTM at different concentrations and primed with LPS before stimulation with nigericin. The copper chelation significantly reduced the secretion of IL-1 β from human PMs isolated from ascites fluid, whereas TNF secretion was unaffected (Fig. 5D). These data indicate that intracellular redox regulation shows notable differences between subsets of monocytes and macrophages in human and mouse. In summary, SOD1 regulates NLRP3 activation in macrophages, but not monocytes, and copper is required specifically for canonical NLRP3 activation in macrophages.

Discussion

Copper chelators are anti-inflammatory and have been used for decades to treat patients with rheumatoid arthritis (19, 59, 60). Unexpectedly, depletion of bioavailable copper did not affect classically secreted proinflammatory cytokine such as TNF, Rantes, and KC, but only reduced unconventionally released caspase-1 dependent cytokines like IL-1. Adding divalent copper abolished the anti-inflammatory properties of TTM completely *in vitro*, confirming its specificity for complexing copper. Together, we provide several lines of evidence that copper chelation is anti-inflammatory by specifically inhibiting canonical NLRP3 inflammasome activation in mice *in vivo* as well as in murine and human peritoneal macrophages *ex vivo*.

In this study, we show that TTM downregulates inflammation by interfering with cellular redox homeostasis. Although ROS are implicated in NLRP3 regulation, the precise mechanism is not understood because the distinct cellular targets of different ROS are not known (61). In this study we report that depleting bioavailable copper inhibits SOD1, recapitulating the phenotype of SOD1-deficient cells (44, 45). In the absence of SOD1, canonical NLRP3 activators induce the glutathionylation of caspase-1 (44). Notably, in this study we show that noncanonical NLRP3-, NLRP1-, NLR4-, and AIM2-dependent inflammasome activation is not ROS sensitive; therefore we propose that additional posttranslational modifications, such as cysteine oxidations, ubiquitinylation, and phosphorylation (62, 63), modulate the activation upstream of caspase-1 in macrophages in a redox-sensitive manner. Interestingly, the activation of NLRP3 by imiquimod was also TTM sensitive, a distinct pathway of NLRP3 activation independent from potassium efflux. Accordingly, the association of NLRP3 with NEK7 and ASC speckling was significantly reduced by TTM, clearly locating the proinflammatory role of copper at the level of the interaction of NLRP3 with NEK7 and ASC or other yet to be defined upstream signaling molecules.

A potential source of intracellular ROS upon stimulation is NOX2; however, macrophages from mice deficient in both SOD1 and CYBB, the catalytic subunit of NOX2, show a phenotype comparable to SOD1-deficient cells, suggesting that NOX2-derived ROS play a dispensable role for the redox-dependent NLRP3 inhibition. The inhibition of NLRP3 by copper chelation is reversible, and was abolished in the presence of a high concentration of the cell-permeable ROS scavenger NAC, pointing toward regulatory reversible redox modifications in this immune cell signaling pathway. On the contrary, SOD1-deficient macrophages did not reach a comparable level of NLRP3 activation in the presence of NAC, suggesting a difference in the quality or quantity of the oxidative modifications arising from an enzymatic long-term defect in ROS degradation.

It has been reported that iNOS inhibits the NLRP3 inflammasome by NO-mediated cysteine nitrosylation (52, 53). In our setting, the redox-sensitive inhibition of NLRP3 was independent of iNOS, suggesting that distinct posttranslational cysteine modifications independently regulate NLRP3. Because reactive nitrogen and oxygen species react with a broad range of molecules, our observations suggest additional redox sensitive cellular targets upstream of NLRP3. Our data therefore indicate that TTM specifically inactivates SOD1, thereby blocking canonical NLRP3 activation by a redox-dependent mechanism.

Interestingly, our data indicate that the requirement for copper is specific to macrophages. Copper chelation did not affect NLRP3 activation in blood-derived monocytes from mice and humans, human blood-derived monocytes, differentiated *in vitro* into macrophage-like cells as well as the myeloid cell lines Mono Mac 6, THP1, or U937. Although we cannot exclude cell-type specific activation mechanisms, the reported differences in intracellular redox homeostasis of monocytes and macrophages (58) replicates the NLRP3-dependent requirement for copper. In this study we used peritoneal human macrophages from patients with ascites with low cellular counts, and excluded neutrophilic and malignant ascites. As expected, we observed large interindividual differences in macrophage counts and cytokine release; however, these primary human macrophages are available in large numbers without the need of *ex vivo* differentiation. We do not know the molecular basis of the differences in copper sensitivity among the tested myeloid cells from human and mouse we describe in this study, and further work will be necessary to investigate this more closely.

At high concentrations, TTM was reported to inhibit copper-dependent enzymes, such as ceruloplasmin and cytochrome oxidase, or downregulate the transcription factors such as NF- κ B and cytokines (20, 64–66). Notably, in our setting up to 25 μ M TTM did not affect NF- κ B-dependent MAPK activation or secretion of classically released cytokines like IL-6 and TNF. At concentrations higher than 50 μ M we observed decreased viability of primary macrophages *ex vivo*, rather than copper-dependent modulation of intracellular signaling or cytokine release. Although, we cannot exclude that NLRP3 inhibition is amplified by additional effects *in vivo*, our data indicate that the anti-inflammatory properties of TTM are mediated by caspase-1-dependent mechanisms, whereas NF- κ B-dependent mechanisms remained largely unaffected.

TTM is an orally active small molecule that is used in the clinic to treat disorders of copper metabolism. *In vivo*, depletion of bioavailable copper attenuated caspase-1 activation, reduced serum concentrations of caspase-1 dependent cytokines, decreased lymphocyte cell death, and increased survival in experimental sepsis model. Protein-based anti-cytokine therapeutics such as anakinra, which blocks the activity of IL-1 α and IL-1 β , are costly and were unsuccessful for the routine treatment of sepsis in the clinic and of some pathologies in NLRP3-dependent systemic inflammatory syndromes (67, 68). Pharmacological blockade of the canonical NLRP3 inflammasome might have several advantages over inhibitors of IL-1 (69): IL-18 and pyroptosis play a pivotal role in many pathological inflammatory conditions and remain unaffected by anti-IL-1 therapies (7, 70).

Because TTM is an approved drug with low toxicity in humans, our data point toward specific therapeutic applications to intervene with NLRP3-dependent pathologies. Besides autoinflammatory and chronic inflammatory conditions, NLRP3 activation is implicated in a growing number of diseases, which were not primarily regarded as inflammatory diseases such as Alzheimer's disease, atherosclerosis, metabolic syndrome, and others (6, 7). Interestingly, TTM has been suggested to have antitumor properties and it

will be interesting to investigate the role of blocking NLRP3 to explain antitumor activity. Because TTM did not block the activation of NF- κ B and the MAPK pathway or other major antimicrobial inflammasomes such as NLR4, NLRP1, and AIM2, it may provide a cost-effective, highly specific, and anti-inflammatory immune modulator with a good safety profile toward opportunistic infections.

Acknowledgments

We thank Soo Peuschel, the Max Planck Institute for Infection Biology, Berlin, for excellent technical assistance. We are grateful to all patients who gave consent for using ascites fluid for research. We thank the medical doctors at the clinic for gastroenterology at the Charité, Berlin who were involved in recruiting patients with ascites, namely S. Tetzlaff, E. Schott, U.-F. Pape, and E. Wiedemann. Eicke Latz and Andrea Stutz (University of Bonn) kindly provided immortalized macrophages used in this study.

Disclosures

The Max Planck Society, which sponsored this study, is public and non-profit, and had no influence on gathering, analyzing, or interpreting the data. The authors have no financial conflicts of interest.

References

- Martinon, F., K. Burns, and J. Tschopp. 2002. The inflammasome: a molecular platform triggering activation of inflammatory caspases and processing of proIL-1 β . *Mol. Cell* 10: 417–426.
- Netea, M. G., F. L. van de Veerdonk, J. W. van der Meer, C. A. Dinarello, and L. A. Joosten. 2015. Inflammasome-independent regulation of IL-1-family cytokines. *Annu. Rev. Immunol.* 33: 49–77.
- Schroder, K., and J. Tschopp. 2010. The inflammasomes. *Cell* 140: 821–832.
- Latz, E., T. S. Xiao, and A. Stutz. 2013. Activation and regulation of the inflammasomes. *Nat. Rev. Immunol.* 13: 397–411.
- Wilson, K. P., J. A. Black, J. A. Thomson, E. E. Kim, J. P. Griffith, M. A. Navia, M. A. Murcko, S. P. Chambers, R. A. Aldape, S. A. Raybuck, et al. 1994. Structure and mechanism of interleukin-1 beta converting enzyme. *Nature* 370: 270–275.
- Lamkanfi, M., and V. M. Dixit. 2012. Inflammasomes and their roles in health and disease. *Annu. Rev. Cell Dev. Biol.* 28: 137–161.
- Dinarello, C. A., A. Simon, and J. W. van der Meer. 2012. Treating inflammation by blocking interleukin-1 in a broad spectrum of diseases. *Nat. Rev. Drug Discov.* 11: 633–652.
- Goldbach-Mansky, R., N. J. Dailey, S. W. Canina, A. Gelabert, J. Jones, B. I. Rubin, H. J. Kim, C. Brewer, C. Zalewski, E. Wiggs, et al. 2006. Neonatal-onset multisystem inflammatory disease responsive to interleukin-1beta inhibition. *N. Engl. J. Med.* 355: 581–592.
- Dinarello, C. A. 2007. Interleukin-18 and the pathogenesis of inflammatory diseases. *Semin. Nephrol.* 27: 98–114.
- Zychlinsky, A., M. C. Prevost, and P. J. Sansonetti. 1992. *Shigella flexneri* induces apoptosis in infected macrophages. *Nature* 358: 167–169.
- Watson, P. R., A. V. Gautier, S. M. Paulin, A. P. Bland, P. W. Jones, and T. S. Wallis. 2000. *Salmonella enterica* serovars Typhimurium and Dublin can lyse macrophages by a mechanism distinct from apoptosis. *Infect. Immun.* 68: 3744–3747.
- Brennan, M. A., and B. T. Cookson. 2000. *Salmonella* induces macrophage death by caspase-1-dependent necrosis. *Mol. Microbiol.* 38: 31–40.
- Wen, H., E. A. Miao, and J. P. Ting. 2013. Mechanisms of NOD-like receptor-associated inflammasome activation. *Immunity* 39: 432–441.
- Bauernfeind, F., E. Bartok, A. Rieger, G. Franchi, G. Núñez, and V. Hornung. 2011. Cutting edge: reactive oxygen species inhibitors block priming, but not activation, of the NLRP3 inflammasome. *J. Immunol.* 187: 613–617.
- Dostert, C., V. Pétrilli, R. Van Bruggen, C. Steele, B. T. Mossman, and J. Tschopp. 2008. Innate immune activation through Nalp3 inflammasome sensing of asbestos and silica. *Science* 320: 674–677.
- Meissner, F., R. A. Seger, D. Moshous, A. Fischer, J. Reichenbach, and A. Zychlinsky. 2010. Inflammasome activation in NADPH oxidase defective mononuclear phagocytes from patients with chronic granulomatous disease. *Blood* 116: 1570–1573.
- van de Veerdonk, F. L., S. P. Smeekens, L. A. Joosten, B. J. Kullberg, C. A. Dinarello, J. W. van der Meer, and M. G. Netea. 2010. Reactive oxygen species-independent activation of the IL-1beta inflammasome in cells from patients with chronic granulomatous disease. *Proc. Natl. Acad. Sci. USA* 107: 3030–3033.
- Zhou, R., A. S. Yazdi, P. Menu, and J. Tschopp. 2011. A role for mitochondria in NLRP3 inflammasome activation. [Published erratum appears in 2011 *Nature*. 475: 122.] *Nature* 469: 221–225.
- Brewer, G. J. 2003. Tetrathiomolybdate anticopper therapy for Wilson's disease inhibits angiogenesis, fibrosis and inflammation. *J. Cell. Mol. Med.* 7: 11–20.
- Juarez, J. C., O. Betancourt, Jr., S. R. Pirie-Shepherd, X. Guan, M. L. Price, D. E. Shaw, A. P. Mazar, and F. Doñate. 2006. Copper binding by tetrathiomolybdate attenuates angiogenesis and tumor cell proliferation through the inhibition of superoxide dismutase 1. *Clin. Cancer Res.* 12: 4974–4982.
- Wei, H., W. J. Zhang, T. S. McMillen, R. C. Leboeuf, and B. Frei. 2012. Copper chelation by tetrathiomolybdate inhibits vascular inflammation and atherosclerotic lesion development in apolipoprotein E-deficient mice. *Atherosclerosis* 223: 306–313.
- Alvarez, H. M., Y. Xue, C. D. Robinson, M. A. Canalizo-Hernández, R. G. Marvin, R. A. Kelly, A. Mondragón, J. E. Penner-Hahn, and T. V. O'Halloran. 2010. Tetrathiomolybdate inhibits copper trafficking proteins through metal cluster formation. *Science* 327: 331–334.
- Brewer, G. J., F. Askari, M. T. Lorincz, M. Carlson, M. Schilsky, K. J. Kluin, P. Hedera, P. Moretti, J. K. Fink, R. Tankanow, et al. 2006. Treatment of Wilson disease with ammonium tetrathiomolybdate: IV. Comparison of tetrathiomolybdate and trientine in a double-blind study of treatment of the neurologic presentation of Wilson disease. *Arch. Neurol.* 63: 521–527.
- Wei, H., B. Frei, J. S. Beckman, and W. J. Zhang. 2011. Copper chelation by tetrathiomolybdate inhibits lipopolysaccharide-induced inflammatory responses in vivo. *Am. J. Physiol. Heart Circ. Physiol.* 301: H712–H720.
- Xu, J., X. Zhang, R. Pelayo, M. Monestier, C. T. Ammollo, F. Semeraro, F. B. Taylor, N. L. Esmon, F. Lupu, and C. T. Esmon. 2009. Extracellular histones are major mediators of death in sepsis. *Nat. Med.* 15: 1318–1321.
- Wang, H., O. Bloom, M. Zhang, J. M. Vishnubhakat, M. Ombrellino, J. Che, A. Frazier, H. Yang, S. Ivanova, L. Borovikova, et al. 1999. HMG-1 as a late mediator of endotoxin lethality in mice. *Science* 285: 248–251.
- Fernandes-Alnemri, T., J. W. Yu, P. Datta, J. Wu, and E. S. Alnemri. 2009. AIM2 activates the inflammasome and cell death in response to cytoplasmic DNA. *Nature* 458: 509–513.
- Hornung, V., A. Ablasser, M. Charrel-Dennis, F. Bauernfeind, G. Horvath, D. R. Caffrey, E. Latz, and K. A. Fitzgerald. 2009. AIM2 recognizes cytosolic dsDNA and forms a caspase-1-activating inflammasome with ASC. *Nature* 458: 514–518.
- Bürckstümmer, T., C. Baumann, S. Blüml, E. Dixit, G. Dürnberger, H. Jahn, M. Planyavsky, M. Bilban, J. Colinge, K. L. Bennett, and G. Superti-Furga. 2009. An orthogonal proteomic-genomic screen identifies AIM2 as a cytoplasmic DNA sensor for the inflammasome. *Nat. Immunol.* 10: 266–272.
- Suzuki, T., L. Franchi, C. Toma, H. Ashida, M. Ogawa, Y. Yoshikawa, H. Mimuro, N. Inohara, C. Sasakawa, and G. Núñez. 2007. Differential regulation of caspase-1 activation, pyroptosis, and autophagy via Ipaf and ASC in *Shigella*-infected macrophages. *PLoS Pathog.* 3: e111.
- Boyden, E. D., and W. F. Dietrich. 2006. Nalp1b controls mouse macrophage susceptibility to anthrax lethal toxin. *Nat. Genet.* 38: 240–244.
- Kanneganti, T. D., N. Ozören, M. Body-Malapel, A. Amer, J. H. Park, L. Franchi, J. Whitfield, W. Barchet, M. Colonna, P. Vandenabeele, et al. 2006. Bacterial RNA and small antiviral compounds activate caspase-1 through cryopyrin/Nalp3. *Nature* 440: 233–236.
- Groß, C. J., R. Mishra, K. S. Schneider, G. Médard, J. Wettmarhausen, D. C. Dittlein, H. Shi, O. Gorka, P. A. Koenig, S. Fromm, et al. 2016. K⁺ efflux-independent NLRP3 inflammasome activation by small molecules targeting mitochondria. *Immunity* 45: 761–773.
- Schmid-Burgk, J. L., D. Chauhan, T. Schmidt, T. S. Ebert, J. Reinhardt, E. Endl, and V. Hornung. 2016. A genome-wide CRISPR (clustered regularly interspaced short palindromic repeats) screen identifies NEK7 as an essential component of NLRP3 inflammasome activation. *J. Biol. Chem.* 291: 103–109.
- He, Y., M. Y. Zeng, D. Yang, B. Motro, and G. Núñez. 2016. NEK7 is an essential mediator of NLRP3 activation downstream of potassium efflux. *Nature* 530: 354–357.
- Shi, H., Y. Wang, X. Li, X. Zhan, M. Tang, M. Fina, L. Su, D. Pratt, C. H. Bu, S. Hildebrand, et al. 2016. NLRP3 activation and mitosis are mutually exclusive events coordinated by NEK7, a new inflammasome component. *Nat. Immunol.* 17: 250–258.
- Wang, S., M. Miura, Y. K. Jung, H. Zhu, E. Li, and J. Yuan. 1998. Murine caspase-11, an ICE-interacting protease, is essential for the activation of ICE. *Cell* 92: 501–509.
- Kayagaki, N., S. Warming, M. Lamkanfi, L. Vande Walle, S. Louie, J. Dong, K. Newton, Y. Qu, J. Liu, S. Heldens, et al. 2011. Non-canonical inflammasome activation targets caspase-11. *Nature* 479: 117–121.
- Kayagaki, N., M. T. Wong, I. B. Stowe, S. R. Raman, L. C. Gonzalez, S. Akashi-Takamura, K. Miyake, J. Zhang, W. P. Lee, A. Muszyński, et al. 2013. Noncanonical inflammasome activation by intracellular LPS independent of TLR4. *Science* 341: 1246–1249.
- Hagar, J. A., D. A. Powell, Y. Aachoui, R. K. Ernst, and E. A. Miao. 2013. Cytoplasmic LPS activates caspase-11: implications in TLR4-independent endotoxic shock. *Science* 341: 1250–1253.
- Hur, J., S. Y. Kim, H. Kim, S. Cha, M. S. Lee, and K. Suk. 2001. Induction of caspase-11 by inflammatory stimuli in rat astrocytes: lipopolysaccharide induction through p38 mitogen-activated protein kinase pathway. *FEBS Lett.* 507: 157–162.
- Doñate, F., J. C. Juárez, M. E. Burnett, M. M. Manuia, X. Guan, D. E. Shaw, E. L. Smith, C. Timucin, M. J. Braunstein, O. A. Batuman, and A. P. Mazar. 2008. Identification of biomarkers for the antiangiogenic and antitumor activity of the superoxide dismutase 1 (SOD1) inhibitor tetrathiomolybdate (ATN-224). *Br. J. Cancer* 98: 776–783.
- Lee, K., M. M. Briehl, A. P. Mazar, I. Batinic-Haberle, J. S. Reboucas, B. Glinsmann-Gibson, L. M. Rimsza, and M. E. Tome. 2013. The copper chelator

- ATN-224 induces peroxynitrite-dependent cell death in hematological malignancies. *Free Radic. Biol. Med.* 60: 157–167.
44. Meissner, F., K. Molawi, and A. Zychlinsky. 2008. Superoxide dismutase 1 regulates caspase-1 and endotoxic shock. *Nat. Immunol.* 9: 866–872.
45. Fridovich, I. 1997. Superoxide anion radical (O₂⁻), superoxide dismutases, and related matters. *J. Biol. Chem.* 272: 18515–18517.
46. Forman, H. J., and M. Torres. 2001. Redox signaling in macrophages. *Mol. Aspects Med.* 22: 189–216.
47. Németh, I., and D. Boda. 1989. The ratio of oxidized/reduced glutathione as an index of oxidative stress in various experimental models of shock syndrome. *Biomed. Biochim. Acta* 48: S53–S57.
48. Cu, A., Q. Ye, R. Sarria, S. Nakamura, J. Guzman, and U. Costabel. 2009. N-acetylcysteine inhibits TNF- α , sTNFR, and TGF- β 1 release by alveolar macrophages in idiopathic pulmonary fibrosis in vitro. *Sarcoidosis Vasc. Diffuse Lung Dis.* 26: 147–154.
49. Liu, Y., W. Yao, J. Xu, Y. Qiu, F. Cao, S. Li, S. Yang, H. Yang, Z. Wu, and Y. Hou. 2015. The anti-inflammatory effects of acetaminophen and N-acetylcysteine through suppression of the NLRP3 inflammasome pathway in LPS-challenged piglet mononuclear phagocytes. *Innate Immun.* 21: 587–597.
50. Palacio, J. R., U. R. Markert, and P. Martínez. 2011. Anti-inflammatory properties of N-acetylcysteine on lipopolysaccharide-activated macrophages. *Inflamm. Res.* 60: 695–704.
51. Hancock, J. T., and O. T. Jones. 1987. The inhibition by diphenyleneiodonium and its analogues of superoxide generation by macrophages. *Biochem. J.* 242: 103–107.
52. Hernandez-Cuellar, E., K. Tsuchiya, H. Hara, R. Fang, S. Sakai, I. Kawamura, S. Akira, and M. Mitsuyama. 2012. Cutting edge: nitric oxide inhibits the NLRP3 inflammasome. *J. Immunol.* 189: 5113–5117.
53. Mishra, B. B., V. A. Rathinam, G. W. Martens, A. J. Martinot, H. Kornfeld, K. A. Fitzgerald, and C. M. Sasseti. 2013. Nitric oxide controls the immunopathology of tuberculosis by inhibiting NLRP3 inflammasome-dependent processing of IL-1 β . *Nat. Immunol.* 14: 52–60.
54. Stehlik, C., S. H. Lee, A. Dorfleutner, A. Stassinopoulos, J. Sagara, and J. C. Reed. 2003. Apoptosis-associated speck-like protein containing a caspase recruitment domain is a regulator of procaspase-1 activation. *J. Immunol.* 171: 6154–6163.
55. Masumoto, J., S. Taniguchi, K. Ayukawa, H. Sarvotham, T. Kishino, N. Niikawa, E. Hidaka, T. Katsuyama, T. Higuchi, and J. Sagara. 1999. ASC, a novel 22-kDa protein, aggregates during apoptosis of human promyelocytic leukemia HL-60 cells. *J. Biol. Chem.* 274: 33835–33838.
56. Stutz, A., G. L. Horvath, B. G. Monks, and E. Latz. 2013. ASC speck formation as a readout for inflammasome activation. *Methods Mol. Biol.* 1040: 91–101.
57. Carta, S., S. Tassi, I. Pettinati, L. Delfino, C. A. Dinarello, and A. Rubartelli. 2011. The rate of interleukin-1 β secretion in different myeloid cells varies with the extent of redox response to Toll-like receptor triggering. *J. Biol. Chem.* 286: 27069–27080.
58. Rubartelli, A. 2012. Redox control of NLRP3 inflammasome activation in health and disease. *J. Leukoc. Biol.* 92: 951–958.
59. Brisset, M., J. P. Pujol, F. Arenzana-Seisdedos, J. L. Virelizier, H. Penfornis, J. Farjanel, A. Rattner, J. Bocquet, R. Beliard, and G. Loyau. 1986. D-penicillamine inhibition of interleukin-1 production: a possible mechanism for its effect on synovial collagen synthesis? *Int. J. Tissue React.* 8: 279–287.
60. Wadhwa, S., and R. J. Mumper. 2013. D-penicillamine and other low molecular weight thiols: review of anticancer effects and related mechanisms. *Cancer Lett.* 337: 8–21.
61. Winterbourn, C. C. 2008. Reconciling the chemistry and biology of reactive oxygen species. *Nat. Chem. Biol.* 4: 278–286.
62. Hoss, F., J. F. Rodriguez-Alcazar, and E. Latz. 2016. Assembly and regulation of ASC specks. *Cell. Mol. Life Sci.* 74: 1211–1229.
63. Rodgers, M. A., J. W. Bowman, H. Fujita, N. Orazio, M. Shi, Q. Liang, R. Amaty, T. J. Kelly, K. Iwai, J. Ting, and J. U. Jung. 2014. The linear ubiquitin assembly complex (LUBAC) is essential for NLRP3 inflammasome activation. *J. Exp. Med.* 211: 1333–1347.
64. Chidambaram, M. V., G. Barnes, and E. Frieden. 1984. Inhibition of ceruloplasmin and other copper oxidases by thiomolybdate. *J. Inorg. Biochem.* 22: 231–240.
65. Mandinov, L., A. Mandinova, S. Kyurkchiev, D. Kyurkchiev, I. Kehayov, V. Kolev, R. Soldi, C. Bagala, E. D. de Muinck, V. Lindner, et al. 2003. Copper chelation represses the vascular response to injury. *Proc. Natl. Acad. Sci. USA* 100: 6700–6705.
66. Pan, Q., C. G. Kleer, K. L. van Golen, J. Irani, K. M. Bottema, C. Bias, M. De Carvalho, E. A. Mesri, D. M. Robins, R. D. Dick, et al. 2002. Copper deficiency induced by tetrathiomolybdate suppresses tumor growth and angiogenesis. *Cancer Res.* 62: 4854–4859.
67. Vanden Berghe, T., D. Demon, P. Bogaert, B. Vandendriessche, A. Goethals, B. Depuydt, M. Vuylsteke, R. Roelandt, E. Van Wonterghem, J. Vandembroecke, et al. 2014. Simultaneous targeting of IL-1 and IL-18 is required for protection against inflammatory and septic shock. *Am. J. Respir. Crit. Care Med.* 189: 282–291.
68. Brydges, S. D., L. Broderick, M. D. McGeough, C. A. Pena, J. L. Mueller, and H. M. Hoffman. 2013. Divergence of IL-1, IL-18, and cell death in NLRP3 inflammasomopathies. *J. Clin. Invest.* 123: 4695–4705.
69. Dinarello, C. A. 2009. Immunological and inflammatory functions of the interleukin-1 family. *Annu. Rev. Immunol.* 27: 519–550.
70. Brydges, S. D., J. L. Mueller, M. D. McGeough, C. A. Pena, A. Misaghi, C. Gandhi, C. D. Putnam, D. L. Boyle, G. S. Firestein, A. A. Horner, et al. 2009. Inflammasome-mediated disease animal models reveal roles for innate but not adaptive immunity. *Immunity* 30: 875–887.